Efficient Design and Analysis of Robust Power Distribution Meshes

Puneet Gupta[a] and Andrew B. Kahng[a,b]
[a] Blaze DFM, Inc., Sunnyvale, CA 94089
[b] CSE Department, University of California at San Diego, La Jolla , CA 92093
(puneet,abk)@blaze-dfm.com

ABSTRACT

With increasing design complexity, as well as continued scaling of supplies, the design and analysis of power/ground distribution networks poses a difficult problem in modern IC design. We propose several closed-form solutions for power distribution network optimization and analysis which explicitly take into consideration the mesh topology of modern power-ground networks. Our analysis and optimization methods have essentially zero runtime for global power grids, and are therefore usable for layout optimization. Experimental validation shows that our IR drop estimation method has almost perfect correlation with true IR drop. Our closed-form sizing solutions save up to 32% area while preserving the peak IR drop; alternatively, we can reduce peak IR drop by up to 33% while preserving the total area of the power distribution network. Our iterated incremental power distribution network improvement technique achieves up to 33% reduction (in one iteration) in peak IR drop over uniformly sized meshes. We also introduce a measure for robustness of power distribution networks to current and process variations.

1. Introduction

Circuits with increasingly higher frequencies and increasingly higher densities have made on-chip power-ground voltage fluctuation very significant. Worst-case voltage drop is increasing with every technology node and easily violates the typical 10% constraint even at the 130nm node [18]. The voltage fluctuation arises from IR drop, $L\frac{di}{dt}$ noise or LC resonance [5]. IR drop may be remedied by sizing up power-ground wire widths and by decreasing their pitch. However, overdesign of the power distribution network consumes valuable clock and global signal routing resources on top-level metal layers.

Area minimization of the power distribution network is a well-studied problem. Early work of Chowdhury et al. [3] solves the nonlinear power distribution problem for networks with tree topologies using the Lagrange multiplier method. [2] solves power distribution networks with general graph topologies by breaking the nonlinear programming problem into two subproblems: one linear program, and one problem with nonlinear objective and linear constraints. [14] linearizes the nonlinear objective in the two-phase approach of [2] by Taylor series expansion around a feasible solution. Tan et al. further simplify the problem by reducing the size of the network in [17]. [16] uses a network simplex algorithm to solve the sequence of linear programs developed in [14]. Model order reduction of the entire power distribution network, followed by a greedy sensitivity-based sizing, is done in [15].

Additional work in power distribution network optimization includes [13] which heuristically solves the original nonlinear program using penalty functions and the conjugate gradient method. [9] deals with the problem of power distribution in the presence of large macro cells. [12] locally sizes a forest-based power distribution network depending on the current estimates. [10] assumes a single-direction power routing to start with, and inserts vias and orthogonal-direction power routing locally as needed. The authors of [6] consider buffer delay change due to IR drop and locally modify the tolerable IR drop to meet timing. They then use the sequence of linear programs approach to solve for power route segment widths. [1] gives a novel way to approximate the power mesh as a space-continuous structure and determine resistivities of uniform horizontal and vertical wiring to meet IR drop budgets. The analysis is fast and useful at the RTL floorplanning stage.

Robustness of power distribution networks to current variations has been addressed in [21], where the authors heuristically try to solve the power distribution network sizing problems when currents have distributions rather than being constant. They show that non-tree topologies may yield better solutions under such constraints. This is consistent with mesh-based power distribution networks design being the commonly accepted design approach to handle current variations. Besides having large runtimes, their approach tends to return solutions which are closer to a tree topology than a mesh topology. [20] propose a power network verification technique by solving a number of linear programs, assuming local and global current bounding constraints. The approach is time consuming and does not account for correlations or the statistical nature of current variations. Neither approach considers the impact of process variations which can cause varying wire width and thickness across the die.

Our work considers a wide outer power ring connected to a global power mesh as the power distribution network topology. Meshes are the accepted way of designing power distribution networks in modern designs [8]. We consider the sizing problem only for the global mesh. Moreover, our analysis is based on time-independent average currents for the power/ground nodes. Thus, a purely resistive model for the mesh is sufficient. Reduction of transient noise in power distribution networks is usually done by adding decoupling capacitances, which we ignore in our analysis. IR drop increases as ones moves toward the center of the chip. This "bull's eye" phenomenon is common in mesh-based power distribution. We make use of this to approximate the power mesh as a collection of distinct equipotential rings and develop closed-form wire sizing solutions. The closed-form expressions permit evaluation of alternative power meshes with negligible computational cost. Important contributions of our work include the following.

- An optimal sizing solution for the one-dimensional power stripe sizing problem;
- closed-form sizing solutions for power grids;
- an incremental improvement technique for power grids;
- a closed-form IR drop calculator for quick IR drop estimation during layout; and
- a measure of robustness of power distribution networks to current and process variations.

The organization of this paper is as follows. In Section 2, we give solution to the one-dimensional power stripe sizing problem as a motivation to the more general 2-D problem. Section 3 describes our three-phase approach to closed-form power grid sizing. Section 4 briefly discusses robustness issues under perturbation of the currents as well as process variations. Experimental results are given in Section 5. Finally we conclude with directions of ongoing research in Section 6.

2. 1-D Case

In this section, we consider a very simple power distribut network topology. It consists of parallel power stripes draw

Proceedings of the 19th International Conference on VLSI Design (VLSID'06)
1063-9667/06 $20.00 © 2006 IEEE

power from a peripheral thick power ring. In such a case, each power stripe can be sized independently.

Consider a power stripe with V_{dd} inputs at one end and n evenly distributed power tap points from which n placed modules draw power. Let these be labeled as $(1,\ldots,n)$ with 1 representing V_{dd} input. Let $i(p,q)$ denote the current flowing from tap point p to tap point q. Also, let $i(j)$ denote the current flowing into the j^{th} tap point. Then

$$i(j-1,j) = i(j,j+1) + i(j) \tag{1}$$

Let $r(p,q)$ denote the resistance of the segment of power stripe between tap points p and q. Let $V(j)$ denote the voltage at tap point j. Then

$$\begin{aligned} V(j+1) &= V(j) - i(j,j+1)\cdot r(j,j+1) \\ &= V(j) - r(j,j+1)\Sigma_{k=j+1}^{n} i(k) \end{aligned} \tag{2}$$

The above equation explains the observed "bull's eye" for IR drop. Equation (2) can be rewritten as follows.

$$V(j+1) = V_{dd} - \sum_{k=1}^{j} i(k)(\Sigma_{m=1}^{k} r(m,m+1)) - (\Sigma_{k=j+1}^{n} i(k))r(j,j+1) \tag{3}$$

Equation (3) also suggests that a nonuniform tapered power stripe which is thicker (i.e., less resistive) toward V_{dd} and thinner away from it will achieve better IR drop reduction with the same total area. To illustrate this more clearly, consider the case of uniform current requirements (i.e., $i(k) = i\ \forall k$). For this case, peak IR drop is given by

$$IR_{peak} = i\sum_{k=1}^{n}(n-k)r(k,k+1) \tag{4}$$

The power distribution optimization problem subject to a peak IR drop constraint then becomes the following.[1]

$$\begin{aligned} &\text{Minimize } \sum_{k=1}^{n}\frac{1}{r(k,k+1)} \\ &\text{subject to } \sum_{k=1}^{n} i(k,k+1)r(k,k+1) \le IR_{peak} \end{aligned} \tag{5}$$

A closed-form solution to this *Min-Area IR Drop Constrained (MAIC)* problem (5) is easily obtained by using Lagrangian multipliers as follows. The Lagrangian is formulated as

$$L = \sum_{k=1}^{n}\frac{1}{r(k,k+1)} + \lambda(\sum_{k=1}^{n} i(k,k+1)r(k,k+1) - IR_{peak})$$

Since the Lagrangian is convex $\bigtriangledown L = 0$ will give the global minimum of the function $\Sigma_{k=1}^{n}\frac{1}{r(k,k+1)}$. Taking partial derivatives we get

$$\frac{-1}{r(k,k+1)^2} + \lambda i(k,k+1) = 0\ \forall k \in [1,n]$$

$$r(k,k+1) = \frac{1}{\sqrt{\lambda}\sqrt{i}(k,k+1)}$$

Substituting in the peak IR drop constraint equation and solving yields the following closed-form solution.

$$r(k,k+1) = \frac{IR_{peak}}{\Sigma_{p=1}^{n}(\sqrt{i(p,p+1)})\sqrt{i(k,k+1)}} \tag{6}$$

Similarly, the *Min-IR Drop Area Constrained (MIAC)* problem is given by

$$\begin{aligned} &\text{Minimize } \sum_{k=1}^{n} i(k,k+1)r(k,k+1) \\ &\text{subject to } \sum_{k=1}^{n}\frac{1}{r(k,k+1)} = G \end{aligned} \tag{7}$$

[1]Note that the total area of the power mesh is directly proportional to the sum of conductances of individual power grid segments. In this paper we use "total conductance" as a measure of area.

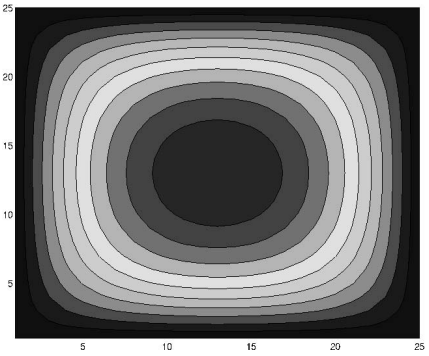

Figure 1: IR drop distribution for a uniform power mesh. The bull's eye at the center is clear. Also note the "circular" equipotential rings.

Formulation (7) can again be solved by substituting $g(k,k+1) = \frac{1}{r(k,k+1)}$ to obtain the following closed-form solution.

$$r(k,k+1) = \frac{\sum_{p=1}^{n}\sqrt{i}(p,p+1)}{G\sqrt{i}(k,k+1)} \tag{8}$$

In this section, we have developed closed-form solutions for two variants of the 1-D power network sizing problem. Power stripes based topologies are no longer very common in modern power distribution networks, except in small macros. More useful 2-D versions of the above problems are discussed in the next section.

3. The 2-D Case

In this section we develop a non-iterative approach to sizing power grids. The approach is an extension of the basic closed-form solutions given in the previous section for the 1-D case.

Analysis of a 2-D power mesh is difficult. Just as in the 1-D case, we expect IR drop to increase toward the center. We begin our discussion with the illustrative example of a square chip, with the current flow as "radially inward". If we divide the layout into concentric rings,[2] then the current flowing into a ring is the sum of currents drawn by the tap points enclosed by the ring. An IR drop map for a 25×25 uniform power grid with uniform current distribution is shown in Figure 1.

The equipotential ring on the power mesh takes the form of a diamond at the center of the (square) chip and gradually changes to a square toward the periphery (since the power mesh is assumed to be connected to a power ring with very low resistance). A reasonable simplification is to assume square equipotential rings all throughout the chip. The edges of each of these rings are the segments of the power mesh. Hence, the total number of rings in a $n\times n$ mesh is $\frac{n-1}{2}$.[3] We take a three-phase approach to 2-D power mesh optimization as follows.

1. *Phase I: Radial Sizing.* We assume a uniform current distribution and solve for optimal sizes for *radial segments* (i.e., segments between two rings).

2. *Phase II: Tangential Sizing.* Since the actual current distribution is not uniform, we divide the layout into *sectors*[4] and redistribute metal along rings between radial segments belonging to different sectors depending on the current requirements of each sector.

3. *Phase III: Circumference Correction.* The assumption of square equipotential rings is accurate only close to the periphery of the chip. The rings are more "circular" or diamond-like toward the center of the layout. This means

[2]If the chip floorplan is not a square, cofocal ellipses can be used.

[3]This assumes odd n. In case of even n the number is $n/2-1$.

[4]We divide the layout into quadrants for this work. Though our experiments assume sector $\approx$ quadrant, the approach is gene and can be easily extended to smaller sectors.

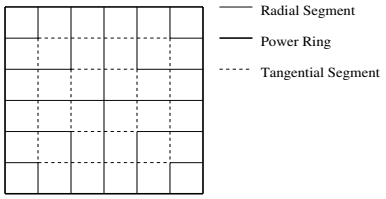

Figure 2: A 5×5 power distribution mesh. Radial and tangential segments are shown.

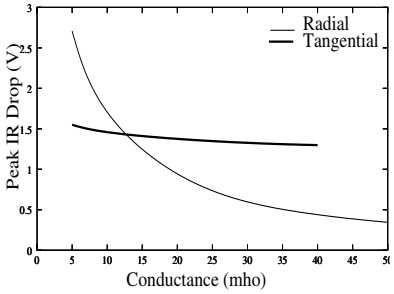

Figure 3: Variation of peak IR drop in a 13×13 power mesh with varying conductance of radial and tangential segments. Note that sizing tangential segments has negligible impact on IR drop.

that there is current flowing through, and hence a voltage drop in, the *tangential segments* of the square rings. We therefore size the tangential segments which lie along the circumference of the rings.

A power distribution mesh with labeled radial and tangential segments is shown in Figure 2.

Figure 3 shows the dependence of peak IR drop on conductance of tangential and radial segments. The dependence of peak IR drop on sizing of tangential segments is weak. This dependence becomes even weaker for larger power grids where equipotential contours look more like squares.

3.1 Radial Sizing

With respect to radial sizing, we note the following.

- No current flows along an equipotential ring. Therefore, segments along the ring can be at maximum resistance (i.e. minimum width).
- The total number of current carrying segments between rings j and $j+1$ (ring $\frac{n-1}{2}$ is closest to the center, and ring 1 is the power ring at the periphery) is $4n-8j$. We assume all of these segments to be carrying equal currents.
- The total current carried by $4n-8j$ segments between rings j and $j+1$ is equal to the current drawn by the modules strictly within the ring j. Following the *1-D* terminology, call this current $i(j, j+1)$. Similarly, let $i(j)$ denote the current drawn by tap points on ring j. Then

$$i(j-1, j) = i(j, j+1) + i(j) \tag{9}$$

Let $r(j, j+1)$ denote the resistance of *each* of the $4n-8j$ segments between the rings j and $j+1$. The voltage drop from ring j to $j+1$ is given by

$$V(j+1) = V(j) - \frac{i(j, j+1)}{4n-8j} \times r(j, j+1) \tag{10}$$

$$= V(j) - r(j, j+1) \sum_{k=j+1}^{\frac{n-1}{2}} \frac{i(k)}{4n-8k}$$

Equation (10) can be rewritten as follows.

$$V(j+1) = V_{dd} - \sum_{k=1}^{j} (i(k) \sum_{m=1}^{k} r(m, m+1)) - r(j, j+1) \sum_{k=j+1}^{\frac{n-1}{2}} \frac{i(k)}{4n-8k} \tag{11}$$

The 2-D *MAIC* problem is given below.

$$\text{Minimize} \sum_{k=1}^{\frac{n-1}{2}} \frac{4n-8k}{r(k, k+1)} \tag{12}$$

$$\text{such that} \sum_{k=1}^{\frac{n-1}{2}} \frac{i(k, k+1)}{4n-8k} r(k, k+1) \leq IR_{peak}$$

A closed-form solution to the *Min-Area IR Drop Constrained (MAIC)* problem for a 2-D mesh is then given by

$$r(k, k+1) = \frac{IR_{peak}(4n-8k)}{\sum_{p=1}^{\frac{n-1}{2}} (\sqrt{i(p, p+1)}) \sqrt{i(k, k+1)}} \tag{13}$$

Similarly, the solution for the 2-D *MIAC* problem is

$$r(k, k+1) = \frac{(4n-8k) \sum_{p=1}^{\frac{n-1}{2}} \sqrt{i(p, p+1)}}{G^R \sqrt{i}(k, k+1)} \tag{14}$$

where G^R is the total conductance allocated to radial segments.

3.2 Tangential Sizing

The second step of our sizing approach redistributes metal along the ring among the radial segments to account for non-uniform distribution of currents. We divide the power grid into quadrants and assume that tap points lying within a quadrant draw current *only* from the power grid segments within that quadrant. We then enforce equal voltage drop between rings. Let i_p^q denote the current drawn by tap points lying in the quadrant q on the ring p. Similarly, let r_p^q be the resistance of each of the $(n-2p)$ segments in the quadrant q in the ring p. Then the metal redistribution constraints are as follows.

$$\frac{i_p^q}{n-2p} r_p^q = V_p$$

$$V_p = \frac{i(p-1, p)}{4n-8p} \times r(p-1, p) \tag{15}$$

where V_p is the voltage drop from ring p to $p-1$ as calculated by the optimal radial sizing solution. If metal-constrained sizing (i.e. *MIAC*) solution is sought, then the constraint is

$$\sum_{q=1}^{4} \frac{1}{r_p^q} = \frac{G_p}{n-2p} \tag{16}$$

where G_p is the total conductance at ring p. In this case the tangential sizing solution is

$$r_p^q = \frac{(n-2p) \sum_{q=1}^{4} i_p^q}{G_p i_p^q}. \tag{17}$$

3.3 Circumference Correction

To correct for the fact that equipotential contours may not look like squares, we heuristically perform local sizing on tangential segments (i.e. the interconnect segments parallel to the power ring). The equipotential contour progresses from being diamond-shaped at the center of the layout to a square.

Geometrically, more correction is required near corners of the square ring to transform it into a diamond. Moreover, the amount of correction required decreases as we progress from the center outward. We model these dependencies as a simple linear function.

$$r(x, y) = r\alpha(x+y+1) \tag{18}$$

where r is the resistance of the radial segment intersecting the given tangential segment, x is the distance of the tangential segment from the nearest corner, and y is the distance of the corresponding ring from the center of the layout. We measure length in number of horizontal or vertical power grid segments. The normalizing factor α affects the conductance of tangential segments only, and hence its impact on IR drop is small. Figure 3 illustrates this weak dependence.

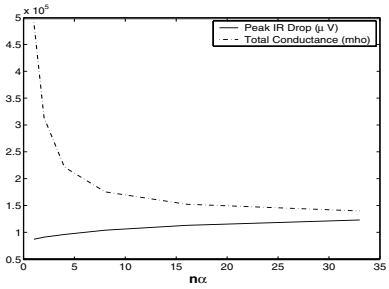

Figure 4: Variation of power mesh area and peak IR drop with α. n denotes the dimension of the square mesh. The variation is plotted for a sample testcase T4 (see Table 3)

.

The total conductance G^{CC} added due to circumference correction can be computed for uniform current requirements:

$$\begin{aligned} G^{CC} &= \frac{8g}{\alpha}\sum_{i=1}^{\frac{n-1}{2}-1}(H_i - H_{\frac{i}{2}}) \\ &\approx \frac{8g}{\alpha}(\frac{n-1}{2}-1)ln(2) \\ &= \frac{4G^R(n-3)ln(2)}{\alpha(n-1)^2} \\ &\approx \frac{4G^R ln(2)}{\alpha(n-1)} \end{aligned} \tag{19}$$

Here, H_k is the k^{th} harmonic number. [5] G^R is the total conductance of radial segments after radial sizing and g is the conductance of each of the radial segments.[6] We use the same expression to approximate G^{CC} for arbitrary meshes as well. Hence, the total conductance of the power mesh is given by

$$G = G^R(1 + \frac{4ln(2)}{\alpha(n-1)}) \tag{20}$$

Equation (20) can be used to determine the required G^R for the *MIAC* sizing solution in Equation (14).

In this section, we have described a simple closed-form approach for sizing power meshes. Section 6 will investigate several degrees of freedom in choosing some parameters (e.g. α)..

4. Incremental Improvement

In this section, we propose a simple area-preserving incremental power distribution network optimization technique. The intuition behind this technique is same as for the radial sizing approach described in the previous section. We want to downsize the power grid segments which lie along the equipotential contours and upsize the ones perpendicular to them. The key difference here is that after a single actual IR drop estimation, the true shape of the equipotential rings becomes apparent and the assumption of "square" equipotential contours can be avoided.

A simple way of doing this sizing is to increase conductance of each segment by a factor proportional to $\frac{\Delta V}{Vdrop_{max}}$ where ΔV is the voltage drop across the segment and $Vdrop_{max}$ is the measured maximum IR drop between any two nodes in the power grid which are connected by a segment. To preserve the area of the power grid, conductances of all the segments can be scaled by a constant factor. Therefore,

$$\begin{aligned} g_{ij}^f &= \beta(1 + \frac{|\Delta V_{ij}|}{Vdrop_{max}})g_{ij}^0 \\ \beta &= \frac{\sum_{i<j} g_{ij}^0}{\sum_{i<j}(1 + \frac{|\Delta V_{ij}|}{Vdrop_{max}})g_{ij}^0} \end{aligned} \tag{21}$$

where g_{ij}^0 is the initial conductance of the segment between nodes i and j and g_{ij}^f is the final conductance after incremental sizing. β is the normalizing factor to preserve the total area. This metal-redistribution can be done after any layout iteration which requires recomputation of the IR drop map. Though, in this work we concentrate our effort on power distribution meshes, this incremental improvement technique can be applied to arbitrary power distribution network topologies.

[5] The k^{th} harmonic number is given by $H_k = \sum_{i=1}^{i=k}\frac{1}{k}$. The first few harmonic numbers are $1, \frac{3}{2}, \frac{11}{6}, \frac{25}{12}, \frac{137}{60}$.

[6] Note that for a mesh with uniform current requirements, the radial sizing solution has all equisized radial segments.

5. Zero-Time IR Drop Analysis

In this section we give a simple heuristic closed-form measure for IR drop at any node based on Section 3. As in Section 3.2, we can subdivide each ring into quadrants. Let VQ_p^q denote the IR drop from the V_{dd} power ring to quadrant q of ring p. Let G_p denote the total conductance of ring p. Then $G_p = \sum_{segment_i \in p}\frac{1}{r_i}$ where r_i is the resistance of the radial segment i in ring p. Similarly we define G_p^q to be the total conductance in quadrant q of ring p. Let I_p be the total current flowing into ring p. I_p is the sum of currents drawn by tap points lying within ring p. Similarly define I_p^q for q^{th} quadrant in ring p. We propose the following expression for VQ_p^q.

$$VQ_p^q = VQ_{p-1}^q + 0.5(\frac{I_p}{G_p} + \frac{I_p^q}{G_p^q}) \tag{22}$$

Then all the tap points lying on ring p in quadrant q are assumed to have same IR drop VQ_p^q. Such a simple measure, if accurate, can be very useful in predicting IR drop and its impact on timing without time-consuming IR drop analysis, especially during layout optimization. Equation (22) can easily be generalized to have further subdivisions of the rings (e.g., use of octants also as sectors) which can yield better accuracy in cases when the current distribution is very nonuniform or the power distribution network is nonuniformly sized.

6. Perturbations and Robustness

We now propose a metric for robustness of a power distribution network with respect to variations. These variations may arise from inaccurate or incomplete peak current estimation or from process variations.

Let $\| A \|_\infty$ denote the infinity norm of the matrix A. $\| A \|_\infty = max_i|a_i|$ if A is a vector. When A is a matrix $\| A \|_\infty = max_i \sum_{j=1}^n |a_{ij}|$. If V_{dd} is set to 0V, then the peak IR drop is given by $\| V \|_\infty$ where V is the solution to $GV = I$. Process variations can manifest as varying width and thickness of metal (e.g., due to CMP effects) across the die leading to variation in the conductance matrix G as well as in the current requirements I. Estimation errors can cause variation in I/

For perturbation matrices E, e such that $(G+E)V' = I + e$ gives the perturbed solution to $GV = I$, an upper-bound on $V' - V$ can be easily derived [19].

$$\frac{\| V' - V \|}{\| V \|} \leq \| G \| \| G^{-1} \| (\frac{\| E \|}{\| G \|} + \frac{\| e \|}{\| I \|}) \tag{23}$$

Note that E has to maintain the structure of the conductance matrix. A simple example of such a matrix can be the scaled version of the original conductance matrix. I.e., $E = \varepsilon G$. $\| G \| \| G^{-1} \|$ is referred to as the *condition number* of G. It is an indicator of robustness of the solution of the IR drop solution with respect to small variations in the conductance matrix as well as currents. Note that this condition number tends to be pessimistic as it does not exploit the structured nature of the perturbations which are allowed in the conductance matrix (e.g., for a mesh, zero entries cannot become non-zero).

In presence of process variations as well inaccurate estimates of peak currents, low condition number of the power mesh conductance matrix becomes an important metric for the power distribution network. Regularization and conditioning procedures are being explored to study this aspect of power distribution network design.

7. Experiments and Results

We validate our results on two artificial power-grid instances with uniform current requirements as well as a testcase dra from the industry. The characteristics of the testcases are g

Testcase	Peak IR Drop (before sizing) (V)	Total Conductance (before sizing) (mho)	Total Conductance (after sizing) (mho)	Measured IR drop (after sizing) (V)	Area Savings (%)
T1	0.11	22080	17425	0.10	21.1
T2	0.21	1140000	775025	0.21	32.0
T3	2.04	11974	8667	1.96	27.6
T4	0.11	217800	160738	0.10	26.2

Table 1: Results of *MAIC* sizing.

Testcase	Peak IR Drop (before sizing) (V)	Total Conductance (before sizing) (mho)	Total Conductance (after sizing) (mho)	Measured IR drop (after sizing) (V)	IR Drop Reduction (%)
T1	0.11	22080	21753	0.08	27.3
T2	0.21	1140000	1139506	0.14	33.3
T3	2.04	11974	11852	1.43	29.9
T4	0.11	217800	215578	0.08	27.3

Table 2: Results of *MIAC* sizing.

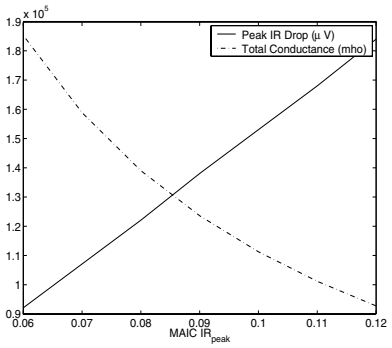

Figure 5: Variation of total conductance and the peak IR drop with varying *MAIC* IR_{peak} for a sample testcase T4.

in Table 3. *MATLAB* [22] is used as the numerical solver to compute exact IR drops.

MAIC sizing underestimates peak IR drop due to the assumption of square equipotential rings. Therefore, a certain guardband is desirable. Variation of conductance and IR drop with the *MAIC* IR_{peak} constraint given to radial sizing is shown in Figure 5 for testcase T4. Comparing Figure 5 and Figure 4 suggests that oversizing the radial segments by lowering $MAICIR_{peak}$ gives more "bang for the buck" as compared to oversizing tangential segments by reducing α. At the same time too large an α is not desirable as it will result in a very non-uniform and unstable power mesh. We choose *MAIC* $IR_{peak} = 0.7 \times$ (Desired peak IR drop) and $\alpha = 0.4$.

The results for *MAIC* sizing are given in Table 2. The simple closed-form three-phase *MAIC* sizing achieves 21% to 32% area reduction over uniformly sized meshes while achieving equal or smaller peak IR drop. For *MIAC* sizing, the radial conductance constraint in Equation (14) is given by $G^R \approx \frac{(n-1)G}{5.9+n}$ for $\alpha = 0.4$. The results for *MIAC* sizing are shown in Table 2. The small differences between intended and actual power grid areas are due to the approximations involved in Equation (20). Our closed-form *MIAC* sizing approach achieves 27% to 33% reduction in peak IR drop with equal or smaller areas of the power grid.

We also run a single iteration of the incremental sizing outlined in Section 4. To illustrate its impact, we perform it on the uniformly sized meshes as given in Table 3 and the results of *MIAC* sizing given in Table 2. The results are shown in Table 4. The approach achieves 12% to 33% improvement in peak IR drop with negligible runtime overhead. The peak IR drops for

Testcase	Peak IR Drop (Uniform) (V)			Peak IR Drop (MIAC) (V)		
	Orig.	Inc.	% Improvement	Orig.	Inc.	% Improvement
T1	0.11	0.09	18	0.08	0.07	12
T2	0.21	0.14	33	0.14	0.13	7
T3	2.04	1.80	12	1.43	1.32	8
T4	0.11	0.10	9	0.08	0.07	12

Table 4: Results of one iteration of incremental sizing. Note that the total conductance is preserved.

Testcase	Peak IR Drop (V)		Correlation	
	Measured	Predicted	Linear	Rank
T1(uniform)	0.11	0.08	0.987	0.988
T1(MAIC)	0.10	0.07	0.969	0.973
T1(MIAC)	0.08	0.06	0.969	0.973
T2(uniform)	0.21	0.17	0.986	0.987
T2(MAIC)	0.21	0.14	0.945	0.951
T2(MIAC)	0.14	0.10	0.945	0.951
T3(uniform)	2.04	1.82	0.980	0.983
T3(MAIC)	1.96	1.35	0.956	0.959
T3(MIAC)	1.43	0.99	0.956	0.959
T4(uniform)	0.11	0.10	0.981	0.983
T4(MAIC)	0.10	0.07	0.956	0.959
T4(MIAC)	0.08	0.05	0.956	0.959

Table 5: Results of fast IR drop analysis. Linear (Pearson) and rank (Spearman) correlation coefficients between the IR drops on the mesh as measured and as predicted are also given.

Testcase	Condition Number		
	Uniform	MIAC	MAIC
T1	499	975	1056
T2	4204	9048	9857
T3	724	1437	1467
T4	1481	2867	3836

Table 6: Robustness of conductance matrices in Table 2 and Table 1.

the *MIAC* sized meshes do not improve by more than 12%. This is just a confirmation of the *MIAC* sizing being fairly close to the optimum.

Results of the closed-form IR drop calculation given in section 4 are shown in Table 5. The high rank correlation coefficients suggest the high fidelity of the simple measure. Moreover, close to 1 linear correlation coefficient suggests a simple linear relationship (e.g. multiply by 1.4) can work well as an approximate IR drop estimator.

Results for robustness analysis for the various conductance matrices are shown in Table 6. It is clear that sized meshes are more non-uniform and less robust. The condition number places a very loose upper-bound on impact of variations. Constructing pathological examples of current and/or process variations such that the upper-bound is attained is still an open problem which we are looking into.

8. Conclusions and Future Work

In this paper, we have presented techniques for sizing and analyzing power distribution meshes. All the techniques are closed-form in nature and hence avoid huge computational overheads of typical mathematical-programming based formulations. We have considered two variants of the power grid sizing problem namely, IR drop constrained (*MAIC*) and area constrained (*MIAC*). For the former, our closed-form sizing achieves 21%-32% area savings over uniformly sized meshes while yielding equal or smaller peak IR drop. Similarly, our *MIAC* sizing approach yields 27%-33% peak IR drop reduction with power mesh areas smaller than corresponding uniformly sized meshes. The proposed incremental sizing approach improves the IR drop of uniformly sized meshes by up to 33% and *MIAC* sized meshes by up to 12% while retaining the same area. This simple incremental improvement can be used in any part of the layout f after an iteration of IR drop analysis has been done (e.g.,

Testcase	Power-grid Size	Horizontal Segment Resistance ($m\Omega$)	Vertical Segment Resistance ($m\Omega$)	Total Conductance (mho)	Peak IR Drop (V)
T1	23×23	50	50	22080	0.11
T2	75×75	10	10	1140000	0.21
T3	33×33	193	172	11974	2.04
T4	33×33	10	10	217800	0.11

Table 3: Characteristics of testcases. T1 and T2 are artificial testcases with uniform current requirements while T3 is drawn from industry. T3 has been derived from a flipchip power distribution network. As a result the IR drop is substantially higher for it in a power ring setup. T4 is derived from T3.

timing verification).

For mesh based power distribution networks, we have proposed a simple IR drop calculator which underestimates the peak IR drop but has almost perfect linear correlation with the true IR drop. As a result, simple scaling of the proposed metric can yield fairly accurate IR drop estimates which can be used during layout optimization (e.g., timing analysis, power distribution network design, etc). We have also given a robustness metric for general power distribution networks to measure sensitivity of the network to current and process variations.

Our ongoing and future work takes several directions as outlined below.

- *Analysis of flipchip based designs.* Many modern designs use flipchip design methodology which places power many power pads on the top of the layout rather than having the conventional power ring. This leads to alleviation of the IR drop problem. Our radial sizing approach can be extended for such cases. The power distribution network then consists of multiple power sources each having concentric diamond-shaped equipotential rings around it. Closed-form solutions for single central power source can be similarly developed but the challenge lies in accounting for interaction between different solder power bumps.
- *Impact of macro cells.* Current layouts may contain a number of macro cells each of which has a power ring of its own, thus disturbing the continuous nature of the power grid. Typically, the macro cells themselves have a finer grained power mesh with a thick power ring. As a result, peak IR drop for the whole layout is likely to improve in presence of such macro cells. We are investigating approaches for sizing and analysis of global power grids in presence of macro cells.
- *Better robustness metrics.* The ∞-norm condition number proposed in this paper gives very pessimistic bounds on impact of perturbations which are not always attainable especially for the case of structured perturbations. Condition numbers for structured perturbations as well per-entry condition numbers (to have better IR drop control for more critical cells in the design for example) are also part of our ongoing research. We are also investigating robustification of conductance matrices using small perturbations.

9. REFERENCES

[1] W. Roethig and T.L. Nguyen, "Estimation of Voltage Drop and Current Densities in ASIC Power Supply Mesh", US Patent 6028440, 2000.

[2] S. Chowdhury, "Optimum Design of Reliable IC Power Networks Having General Graph Topologies", *Proc. IEEE/ACM Design Automation Conference*, 1989, pp. 787-790.

[3] S. Chowdhury and M.A. Breuer, "Optimum Design of IC Power/Ground Nets Subject to Reliability Constraints", *IEEE Transactions on Computer Aided Design of Integrated Circuits and Systems*, 7(7) (1988), pp. 787-796.

[4] A. Dalal, L. Lev and S. Mitra, "Design of an Efficient Power Distribution Network for the UltraSPARC-I Microprocessor", *Proc. IEEE International Conference on Computer Design*, 1995, pp. 118-123.

[5] S. Lin and N. Chang, "Challenges in Power-Ground Integrity", *Proc. IEEE/ACM International Conference on Computer-Aided Design*, 2001, pp. 651-654.

[6] A. Mukherjee, K. Wang, L.H. Chen and M. Marek-Sadowska, "Sizing Power/Ground Meshes for Clocking and Computing Circuit Components", *Proc. IEEE/ACM Design Automation and Test in Europe*, 2002, pp. 176-183.

[7] W.S. Song and L.A. Glassner, "Power Distribution Techniques for VLSI Circuits", *IEEE Journal of Solid-State Circuits*, SC-21(1) (1986), pp. 150-156.

[8] A. Dharchoudhury, R. Panda, D. Blaauw and R. Vaidyanathan, "Design and Analysis of Power Distribution Networks in PowerPC Microprocessors", *Proc. IEEE/ACM Design Automation Conference*, 1998, pp. 738-743.

[9] X. Wu, C. Qiao and X. Hong, "Design and Optimization of Power/Ground Network for Cell-Based VLSIs with Macro Cells", *Proc. IEEE/ACM Asia South Pacific Design Automation Conference*, 1999, pp. 21-24.

[10] T. Mitsuhashi, "Method and Apparatus for Power-Source Wiring Design of Semiconductor Integrated Circuits", US Patent 5404310, 1995.

[11] D.R. Brasen and B.S. Seiler, "Method for Sizing Widths of Power Busses in Integrated Circuits", US Patent 5349542, 1994.

[12] S. Ito, "Method of Automatically Optimizing Power Supply Network for Semi-Custom Made Integrated Circuit Device", US Patent 5648910, 1997.

[13] X. Wu, X. Hong, Y. Cai, C.K. Cheng, J. Gu and W. Dai, "Area Minimization of Power Distribution Network Using Efficient Nonlinear Programming Techniques", *Proc. IEEE/ACM International Conference on Computer-Aided Design*, 2001, pp. 153-157.

[14] X.-D. Tan, C.-J. R. Shi, D. Lungeanu, J.-C. Lee and L.-P. Yuan, "Reliability-Constrained Area Optimization of VLSI Power/Ground Networks Via Sequence of Linear Programmings", *Proc. IEEE/ACM Design Automation Conference*, 1999, pp. 78-83.

[15] H. Su, K.H. Gala and S.S. Sapatnekar, "Fast Analysis and Optimization of Power/Ground Networks", *Proc. IEEE/ACM International Conference on Computer-Aided Design*, 2000, pp. 477-480.

[16] T.-Y. Wang and C. C.-P Chen, "Optimization of the Power/Ground Network Wire-Sizing and Spacing Based on Sequential Network Simplex Algorithm", *Proc. IEEE International Symposium on Quality Electronic Design*, 2002, pp. 157-162.

[17] S. X.-D. Tan and C.-J. Shi, "Efficient Very Large Scale Integration Power/Ground Network Sizing Based on Equivalent Circuit Modeling", *IEEE Transactions on Computer Aided Design of Integrated Circuits and Systems*, 22(3) (2003), pp. 277-284.

[18] A.H. Ajami, K. Banerjee, A. Mehrotra and M. Pedram, "Analysis of IR-Drop Scaling with Implications for Deep Submicron P/G Network Designs", *Proc. IEEE International Symposium on Quality Electronic Design*, 2003.

[19] G.W. Stewart and J.-G. Sun, *Matrix Perturbation Theory*, Academic Press Inc. ,1990.

[20] D. Kouroussis and F.N. Najm, "A Static Pattern-Independent Technique for Power Grid Voltage Integrity Verification", *Proc. IEEE/ACM Design Automation Conference*, 2003, pp. 99-104.

[21] S. Boyd, L. Vandenberghe, A. El Gamal and S. Yun, "Design of Robust Global Power and Ground Networks", *Proc. IEEE/ACM International Symposium on Physical Design*, 2001, pp. 60-65.

[22] *http://www.mathworks.com*